BULLETIN OF THE POLISH ACADEMY OF SCIENCES
TECHNICAL SCIENCES, Vol. 62, No. 3, 2014
DOI: 10.2478/bpasts-2014-0051

Synthesis, characterization and catalytic properties of SAPO-11 molecular sieve synthesized in hydrothermal media using di-isopropylamine as template

T. CHELLAPPA[1*], M. JOSÉ FONSECA COSTA[2], W.A. NASCIMENTO[3], L. FERREIRA DE LIMA[1], Í. ALMEIDA BASSAN[2], M. TAVARES[2], V.J. FERNANDES JR.[2], A. MENEZES[1], L. GUILHERME MEIRA[1], J. TELÉSFORO NÓBREGA DE MEDEIROS[1], and R. MARIBONDO DO NASCIMENTO[1]

[1] Department of Mechanical Engineering, Federal University of Rio Grande do Norte, P.O. Box 1662 59078-970, Natal/RN, Brazil
[2] Department of Chemistry, Federal University of Rio Grande do Norte, 59078-970, Natal/RN, Brazil
[3] Department of Biology, Federal University of Rio Grande do Norte, 59078-970, Natal/RN, Brazil

Abstract. A microporous SAPO-11 Molecular sieve was successfully synthesized by the hydrothermal method, using a single agent, as an organic template: di-isopropylamine (DIPA). The obtained solid was calcined at 550°C for three hours, after which the flow of nitrogen was exchanged for that of synthetic air and submitted for another ten hours of calcination, so as to remove the single agent: di-isopropylamine, which after the removal of the template could be observed by the high crystallization of the sample. Furthermore, the molecular sieve was characterized by XRD, SEM, TG-DTG and N_2 adsorption desorption (BET analysis). The obtained catalyst proved to have a high potential catalytic activity and selectivity, through the obtained characterization results, exhibiting good hydrothermal stability. The catalytic performance of SAPO-11 was tested by the deactivation/regenerability of the coked sample, furthered by cracking of n-hexane reaction and high olefins selectivity was obtained.

Key words: microporous materials, SAPO-11, characterization, catalytic activity, molecular sieves.

1. Introduction

Silicoaluminophosphate molecular sieves denoted as SAPO were synthesized by Lok et al. [1, 2] and composed of strictly alternating AlO_4, PO_4 and SiO_4 tetrahedra. Among these SAPO materials, SAPO-11 has the $AlPO_4$-11 (AEL) topology, comprising of unidirectional, non-intersecting, 10-membered ring channels. With elliptical pore apertures of 0.39–0.63 nm [3].

Silicoaluminophosphates are an important class of adsorbents and catalytic materials generated by the introduction of silicon into its respective aluminophosphate phase framework [4–6]. This isomorphic substitution can occur by a replacement of one aluminum by one silicon (SM1), replacement of one phosphorous by one silicon (SM2), or replacement of aluminum-phosphorous pairs by two silicon (SM3).

The catalytic activity and medium acid sites can be generated in SAPO-11 by isomorphic substitution of silicon or transition metals for aluminum and phosphorous on its surface [7–11]. And many research works have been reported relating to the synthesis and crystallization mechanism [12–14].

It is well known that template plays important roles in the synthesis of molecular sieves, such as structure-directing, space-filling and charge-compensating roles [15–17]. One template may produce molecular sieves with different structures by varying the synthetic conditions; and one type of molecular sieve could also be synthesized in the presence of different organic templates [16]. The elemental composition, local microscopic structure and morphology of one specific molecular sieve may change with the use of different templates.

Therefore, SAPO-11 molecular sieve is usually synthesized through traditional static hydrothermal crystallization at 160–220°C using a single agent, such as, di-isopropylamine as structure-directing template, H_3PO_4 as source of P, pseudoboehmite as source of Al and silica sol or tetraethylorthosilicate (TEOS) as source of Si. The crystal morphology of SAPO-11 synthesized by the traditional hydrothermal method often exhibits pseudospherical or orthorhombic aggregates of cubic plates ranging from 3 to 10 μm owing to the rapid congregativeness of crystal nuclei [18–20]. In this present work, the SAPO-11 molecular sieve after the hydrothermal method of synthesis was washed with distilled H_2O, dried and calcined with the intention of easing the removal of the template agent from the micrpores of the catalyst, and furthermore submitted to characterization through: XRD, SEM, FT-IR TG-DTG and N_2 Adsorption desorption (BET analysis). The catalytic performance of the sample in deactivation/regenerability of the coked sample, furthered by cracking of n-hexane reaction was also tested. The aim of this present work was to obtain results that indicate that the SAPO-11 molecular sieve has a high potential in relation to its catalytic activity and selectivity.

*e-mail: thiagochellappa@yahoo.com.br

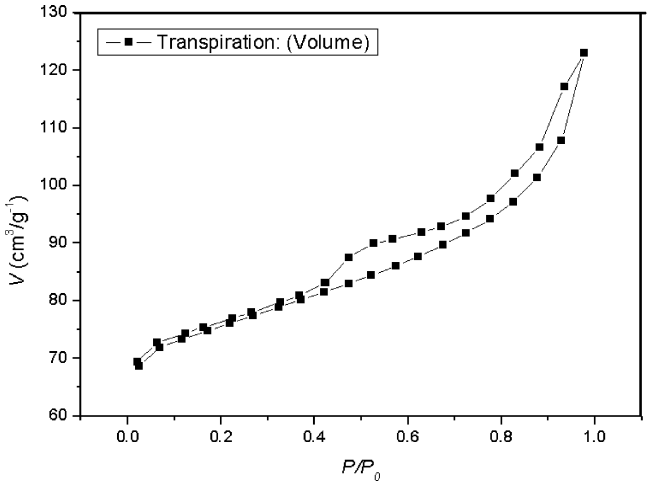

Fig. 1. Isotherms of adsorption of N_2 and distribution of pore diameter of microporous SAPO-11

Table 1
Physicochemical properties of SAPO-11 molecular sieve

Sample	A_{BET} [m^2g^{-1}]			Microporous Volume [ml/g]	Pore size [Å]	Pore diameter [nm]	Relative crystallinity [%]
	S_{total} [a]	S_{micro} [b]	S_{ext} [c]				
SAPO-11	239	173.11	65.9	0.088	14	1.4	85.9

[a] total surface area; [b] microporous surface area; [c] external surface area

2. Experimental

2.1. Preparation of the SAPO-11 molecular sieve. The SAPO-11 molecular sieve sample was synthesized by the hydrothermal method the reagents used in the synthesis were pseudoboehmite (70 wt% Al_2O_3), orthophosphoric acid (85 wt% H_3PO_4), Si colloidal gel (30% SiO_2), fumed silica (99% SiO_2) and di-isopropylamine (98% DIPA). Initially pseudoboehmite was dispersed in two thirds of the distilled H_2O (47.66 ml), used as a solvent, under constant magnetic stirring for 30 min, afterwards the orthophosphoric acid was diluted in the remaining H_2O (23.83 ml) being added dropwise, remaining for a further 120 min under stirring.

After this period of time, di-isopropylamine was added to the mixture and stirring continued for a further 60 min when the silica was finally added to the synthesis gel, thus completing the stirring after another 40 min. The quantities of each precursor were measured on an analytical balance (Mettler model). For the preparation of an amount of 100 grams of gel (20.66 g of SAPO-11) the following quantities of reagents were necessary DIPA: 7.55 ml; H_3PO_4: 7.49 ml; SiO_4: 1.65 g; Pseudoboehmite: 8.59 g and distilled H_2O: 71.49 ml.

After completing these procedures, the pH of the gel was measured (8) and the final mixture was sealed in a stainless steel autoclave lined with polytetrafluoroethylene (PTFE) and heated for 200°C for 72 h. Finally the as-synthesized products were washed, centrifuged, filtered, dried at 120°C for 3 h, and then calcined at 550°C for another 10 h in air in order to remove the template.

2.2. Characterization. Powder X-ray diffraction patterns (XRD) was recorded on a SHIMADZU-6000 diffractometer, using the CuKa ($k = 1.5404$ Å) radiation at 40 kV and 30 mA with a scanning rate of 2° 2θ.min^{-1}.

The morphology of the products was examined by a Cambridge S-360 scanning electron microscope (SEM). The composition of the final material was determined by sequential X-ray Fluorescence Spectrometer (SHIMADZU, XRF-1800).

The characterization of surface area and pore volume of the SAPO-11 molecular sieve was performed by using N_2 adsorption-desorption at −196°C, in a NOVA 2000 Quantachrome Instruments surface are & pore size analyzer automatic adsorption apparatus. Samples were outgassed at 350°C for 3 h under a vacuum of 1.33×10^{-3} Pa prior to N_2 physisorption. The BET surface areas of the samples (A_{BET}) were calculated by applying the BET equation [21] to N_2 adsorption data in relative vapor pressure (p/p_0) range of 0.05–0.30. The cross-sectional area of N_2 molecule was taken as 14.0 Å The pore volume (Vp) of the catalysts were obtained by extrapolating the upper parts of the desorption branches of the N_2 adsorption–desorption hysteresis loops to the relative pressure (p/p_0) of 1.0 [22]. The mean pore diameter (d) of the SAPO-11 molecular sieves were calculated with $d = 4Vp/A_{BET}$ assuming a cylindrical pore model. The pore size distributions in the pore diameter range of 1.5–100 nm of the samples were obtained by applying the expanded BJH equations [23] to the N_2 desorption branches of the hysteresis loops. Size distribution of microspores was determined by the HK method, and the external surface areas of the samples were calculated by the t-plot method.

The thermal analysis was performed on a Mettler Toledo TGA/SDTA 851 analyzer with the temperature programmed-rates of 5, 10 and 20°C.min^{-1} under air flow.

2.3. Catalyst Testing . The catalytic performance of SAPO-11 was tested by the deactivation/regenerability of the coked sample, furthered by cracking of n-hexane reaction. It was carried out with a fixed-bed reactor at atmospheric pressure. 200 mg of catalyst was loaded into the reactor. The sample was pretreated with nitrogen flow of 35 ml /min, at 400°C for 2 h. Upon activation of the catalyst, the vapors of n-hexane were encompassed to reach the micro-reactor where the reaction occurred. The reactor operated at a ratio F/W (molar flow of reactant per gram of catalyst) of 0.85 mmol/hg. The volume flows were measured at the output of the reactor by a digital flow meter model ADM 1000 (Micronal). The products were analyzed on-line by a Varian GC3800 gas chromatograph equipped with a FID detector and a Poraplot Q-HT capillary column.

3. Results and discussion

3.1. Microstructural properties XRD. The X-ray powder diffraction patterns of the sample synthesized by hydrothermal media, SAPO-11 are shown in Fig. 2. The characteristic peaks of the SAPO-11 phase (i.e. 2u = 8.1°, 9.8°, 12.8°, 16.1°, 21.9°, 22.2°, 22.4°, 23.5°) were observed in many different samples in scientific literature, and were very similar to those reported for the currently analyzed SAPO-11 sample [24, 25].

Among other peaks that were observed, one in 9.8° was reported, indicating that the samples had some slight phase impurities, these trace impurities arise from non-ideal synthesis conditions. However, the high intensity of XRD peaks indicated that the sample was highly crystalline. A result that was furthermore corroborated when the cristallinity of the sample was found to be 95%. The X-ray powder diffraction patterns identified that the sample synthesized from aqueous media possessed the AEL structure.

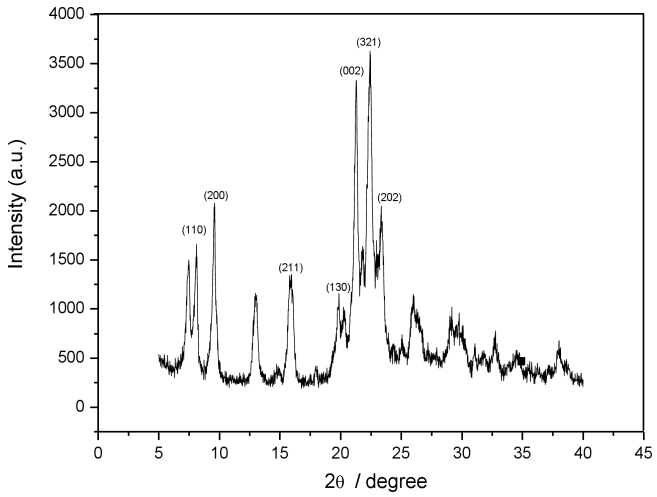

Fig. 2. XRD Pattern of a SAPO-11 molecular sieve synthesized by the hydrothermal method

Morphological properties. SEM. The morphology of the sample synthesized by hydrothermal media was characterized by the scanning electron micrographs. As shown in Fig. 3, there was little difference in the crystal morphology between SAPO-11 (c) and SAPO-11 (nc). Both of them exhibited pseudo-spherical aggregates ranging from 7 to 10 μm assembled from cubic plate small crystallites. Another interesting observation that could be made is that an orthorhombic geometrical pattern was observed in some of the micrographs, which denotes the microporous structure of the SAPO-11 sample.

Surface area. The specific surface area (BET), microporous surface area and external surface area of the samples are listed together with the total microporous volume, mean pore diameter, pore size and relative cristallinity of the samples that were measured. During crystallization, Si was released slowly from the silica sol and the organic phase to the aqueous phase, so that the Si content of SAPO-11 was low. During the synthesis of SAPO-11, the framework of SAPO-11 is identical to that of AlPO-11 with AEL type structure. The cavity volume consists of nonintersecting elliptical 10 membered ring pores of 0.39 nm_0.63 nm. The N_2 adsorption-desorption isotherm curves showed that the samples synthesized from hydrothermal media had a well-defined adsorption-desorption hysteresis loop above the relative vapor pressure of 0.3, indicating the existence of some mesoporous materials that originated from the secondary pores. The N_2 adsorption–desorption hysteresis loop of this material belongs to type E of de Boer's classification [26].

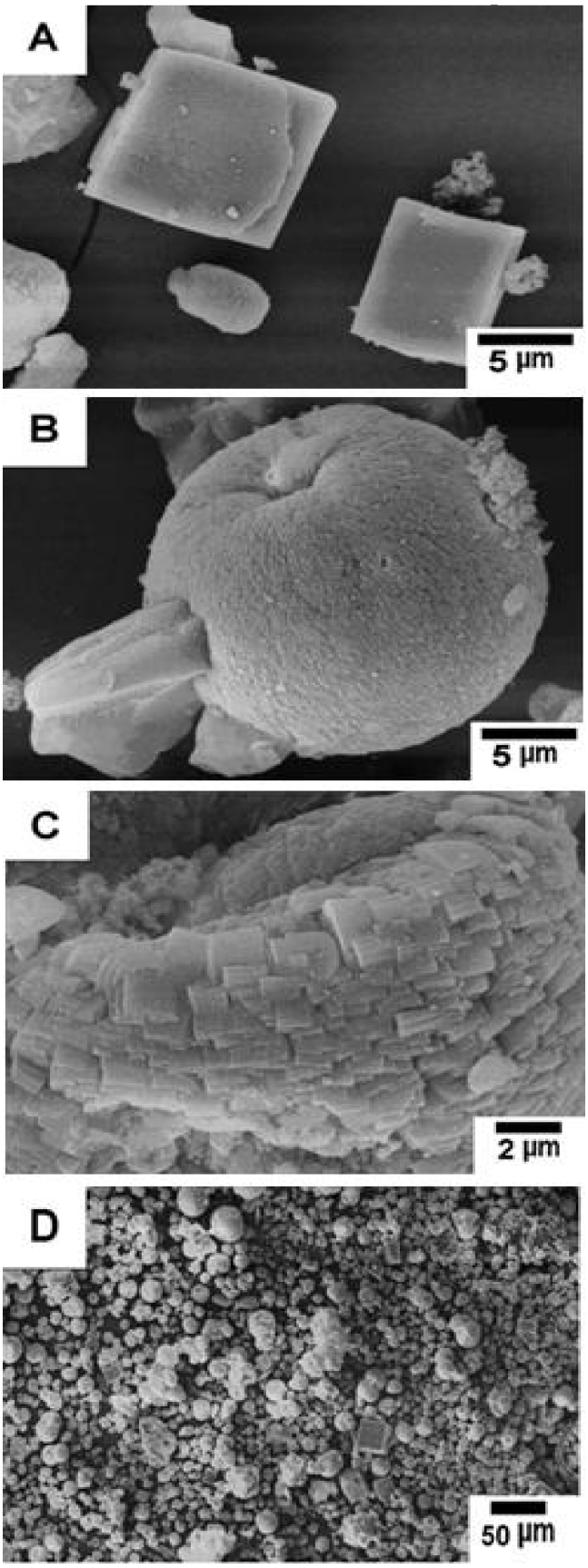

Fig. 3. SEM images of a SAPO-11 molecular sieve synthesized by the hydrothermal method

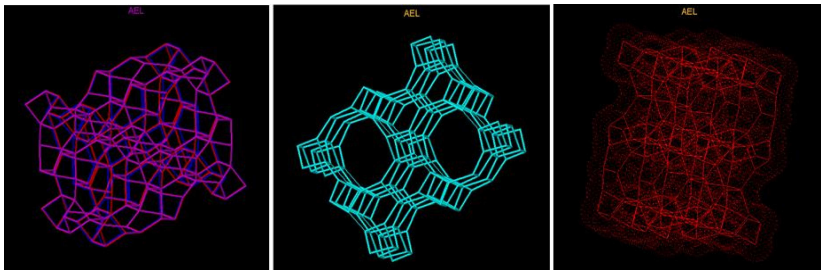

Fig. 4. Schematic array of zeolites with AEL structure, such as SAPO-11

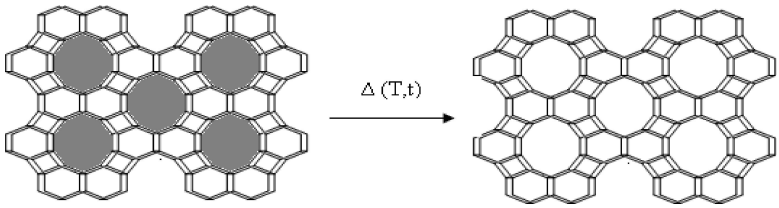

Fig. 5. Representative sketch of the removal of the template from the microporous materials

3.2. Thermal analysis. Calcination is a very important step in achieving microporous materials of high quality, such as the silicoaluminophosphate type, this phase consists in removing the template di-isopropylamine. Thermogravimetry is a technique used to determine the optimum calcinations temperature, designed to remove all the organic material and maintain the preservation of an orderly structure. A representative scheme of the removal of the template, typically encountered in this microporous material could be seen in Fig. 5.

Figure 6 shows the TG and DTG curves for the non-calcined sample of SAPO-11 on three separate heating rates (β = 5, 10 and 20°C.min^{-1}). It could be observed in the curves three events of mass loss. These events are attributed to:

- In the range of 30–150°C – desorption of intracristaline water;
- In the range of 150–300°C – removal of physically adsorbed template;
- In the range of 300–400°C – was associated with decomposition of the di-isopropylamine molecule in propene and ammonia (Hoffman degradation).

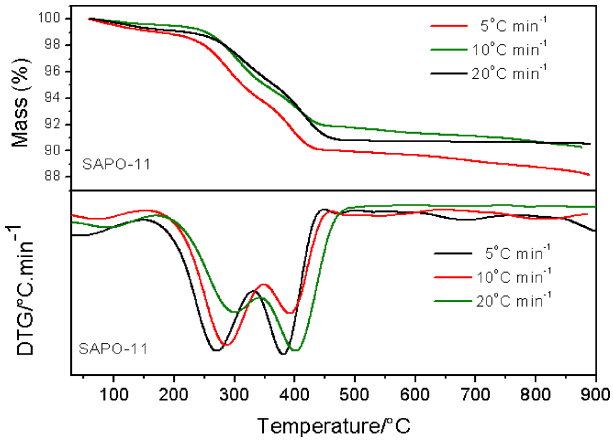

Fig. 6. TG/DTG curves of non-calcined SAPO-11 sample obtained at different heating rates

The difference of mass loss percentage between the materials on the first phase indicates the removal of water from the micropores, and is attributed to the humidity that the sample was exposed prior to thermogravimetric analysis. In relation to the second phase of mass loss in the SAPO-11 sample, the percentage is related to the desorption of the di-isopropylamine (DIPA) template [22].

Figure 7 shows the curve of apparent activation energy for the DIPA removal of SAPO-11 and its rate: 158.91 kJ.mol^{-1}.

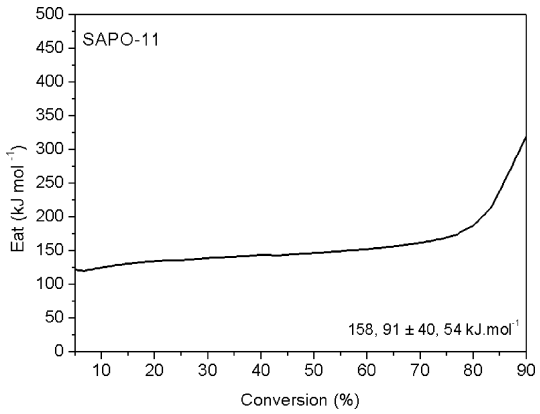

Fig. 7. Apparent activation energy for DIPA removal of SAPO-11

3.3. Catalytic tests. The catalytic tests, such as the n-hexane cracking were carried out to evaluate the conversion and selectivity of the catalyst and the deactivation of SAPO-11 through deposition of carbonaceous products (coke) in the micropores of the catalyst.

According to the chromatograms reactions with SAPO-11 obtained the following products: ethylene, isobutane, 1-butene, n-butane, 2-butene-trans, cis-2-butenes, n-pentane and isopentane. In n-hexane cracking reactions, the lifetime span is very small during the catalytic cycle, thus causing the deactivation of the catalysts under study as expected for the application of kinetic study regeneration [27]. Figures 8 and 9 showed alternate graphics of conversion and selectivity of products for the catalytic tests.

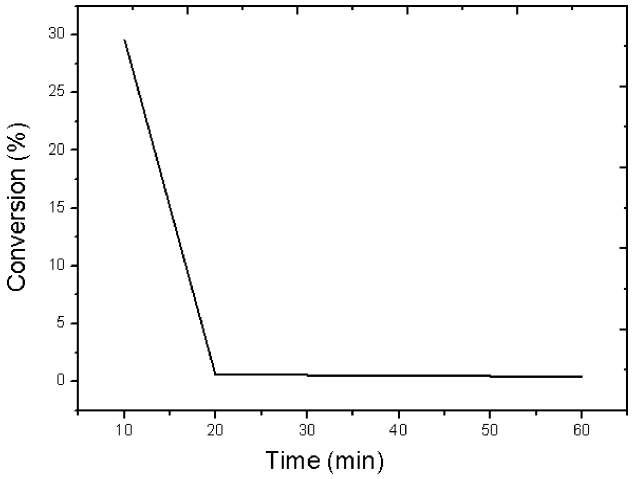

Fig. 8. Conversion as a function of reaction time for the sample of SAPO-11

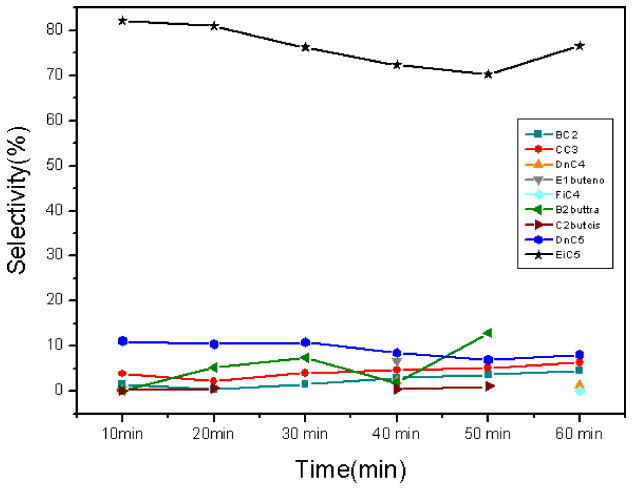

Fig. 9. Selectivity of products in function of reaction time of SAPO-11

Figure 9 shows the results of selectivity for C3 and C4 respectively, which indicate that the production of propane is much higher than that of propylene for all samples. In the case of C4 there is no formation of olefins, only butane and isobutane. Achieving these results are due to reactions of hydrogen transfer or hydride of coke formed, migrating to the active acid sites and saturating the olefins (such as carbenium ion), preferably forming alkanes. The Fig. 9 also shows, through data on the selectivity of the reaction products in function of the reaction time, how was the ratio of the total paraffins in relation to the total olefins (r(P/O)), n-butane to isobutane over (r(n-but/isob)), ratio of 1-butene and 2-butenes (r(1-but/2but)) and the relationship between 2-butene-trans and cis-2-butene (r(trans/cis)).

The rates of the paraffins in relation to the olefins were always below one, indicating a predominance of olefinic products such as: 1-butene, 2-butene-trans and cis-2-butene. It was also observed high n-butane/isobutane reasons indicating that isomerization reactions of chain n-butane occurred on a small scale. This can also be confirmed by viewing the selectivity graphs of products, where the isobutane always appears as product in smaller quantities. Regarding the ratio of 1-butene and 2-butenes and 2-butene-trans and 2-butene-cis, one can observe that there was in the majority of cases the following selectivity rule: propane $>$ isobutane $>$ n-butane $>$ isopentene $>$ n-pentene $>$ 2-butene-trans $>$ cis-2-butene $>$ n-pentane $>$ isopentane.

3.4. Regeneration kinetics. The regeneration study of the coked catalyst was carried in a thermobalances, Mettler TG/SDTA 851 using three different heating rates ($\beta = 5$, 10 and 20°C.min^{-1}) with air flow of 120 cm$^3_{\text{min}}-1$ and the coked catalyst mass of 0.01 g for this experiment. The TG/DTG curves of the coked sample are shown in Fig. 10. The first thermogravimetric analyses of the material were carried out to determine the ideal temperature of removal of the coke deposited on the micropores of the silicoaluminophosphate. The removal of light organics at the first phase ranges from 30–150°C, the second phase ranges from 400–750°C refers to the decomposition of coke deposited in the pores of the catalysts. The ideal temperature is 509.06°C for a period of 1 h.

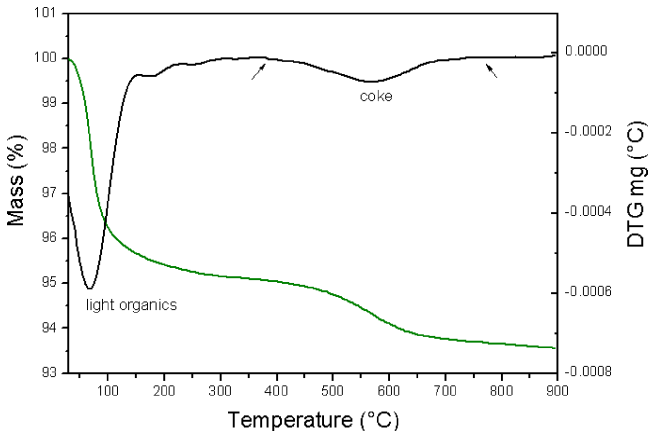

Fig. 10. TG/DTG Curves for Coked SAPO-11with heating rate $\beta = 10$°C.min^{-1} with a continuous air flow of 120 cm^3 min^{-1}

The greater activity obtained with SAPO-11 nanocrystals can be explained by their smaller crystals size. It is observed that the conversion time decreases considerably as a function of temperature. Thus it is possible to predict the temperature for the removal of coke as a function of time and consequently enabling the estimation of the optimum temperature for the removal of coke as described in Table 3.

Coke deposition is often studied as a function of time-on-stream. The interpretation of the measured coke as a function of time-on-stream is a good parameter for describing the coke depositions in different conditions. A lower space velocity resulted in a higher coking rate, as a result of high average of concentration of olefins. It indicates that the rate of coke deposition is related to the concentration of olefins. Furthermore, it was observed that for the removal of 90% of coke deposited on the catalyst during a period of 1 h, it was necessary to heat the sample of coked SAPO-11 to 509.06°C under an air atmosphere.

Table 2
Temperatures for the DIPA (C) removal of (SAPO-11)

Time [min]	10%	20%	30%	40%	50%	60%	70%	80%	90%	95%	99%
10	160	167	188	201	213	224	236	251	326	362	392
20	151	159	179	192	203	214	226	241	320	358	389
30	147	154	174	187	198	209	220	236	316	356	387
40	143	150	170	183	195	205	217	232	314	354	386
50	140	147	167	180	192	202	214	229	312	353	385
60	138	145	165	178	189	200	211	227	310	352	384
70	137	144	163	176	188	198	209	225	309	351	383
80	135	142	162	175	186	196	208	223	307	351	383
90	134	141	160	173	184	195	206	221	306	350	382
100	133	139	159	172	183	193	205	220	305	349	382
110	131	138	158	171	182	192	204	219	305	349	381
120	130	137	157	170	181	191	203	218	304	348	381

Table 3
Temperature (°C) for removal of coke as a function of time at different conversions

Time (min)	10%	20%	30%	40%	50%	60%	70%	80%	90%
10	–	446.57	477.74	500.06	518.31	535.00	551.36	568.48	589.43
20	–	431.49	459.62	479.16	494.40	509.12	523.12	538.12	556.45
30	–	422.96	449.41	467.45	481.07	494.73	507.48	521.36	538.31
40	–	417.03	442.34	459.35	471.89	484.84	496.75	509.88	525.91
50	–		436.95	453.20	464.92	477.35	488.63	501.20	516.55
60	–	–	432.61	448.25	459.33	471.33	482.12	494.25	509.06
70	–	–	428.98	444.11	454.66	466.32	476.70	488.47	502.84
80	–	-	425.86	440.57	450.67	462.03	472.07	483.53	497.53
90	–	–	423.14	437.47	447.18	458.29	468.04	479.23	492.91
100	–	–	420.72	434.72	444.09	454.97	464.46	475.42	488.82
110	–	–	418.54	432.25	441.31	452.00	461.26	472.01	485.16
120	–	–	416.57	430.01	438.80	449.31	458.36	468.93	481.84
130	–	–	–	427.97	436.50	446.85	455.71	466.11	478.82
140	–	–	–	426.09	434.39	444.59	453.27	463.52	476.05
150	–	–	–	424.34	432.44	442.49	451.02	461.13	473.48
160	–	–	–	422.72	430.62	440.55	448.93	458.90	471.10
170	–	–	–	421.20	428.92	438.73	446.97	456.82	468.87
180	–	–	–	–	–	–	–	–	–

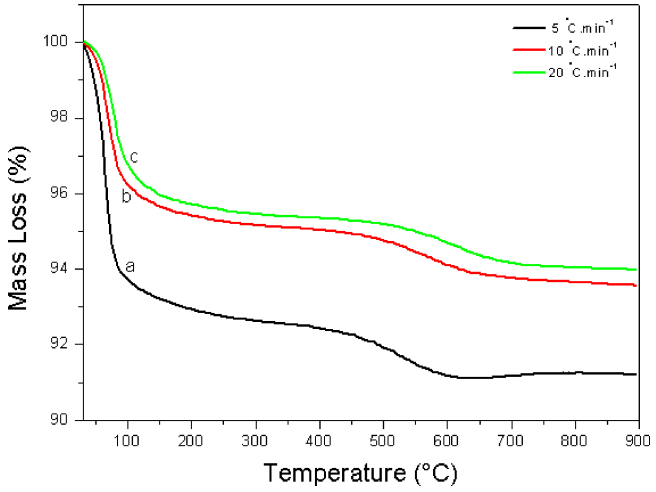

Fig. 11. TG curves of the coked SAPO-11 sample with heating rates: a – 5°C.min^{-1}, b – 10°C.min^{-1}, c – 20°C.min^{-1}

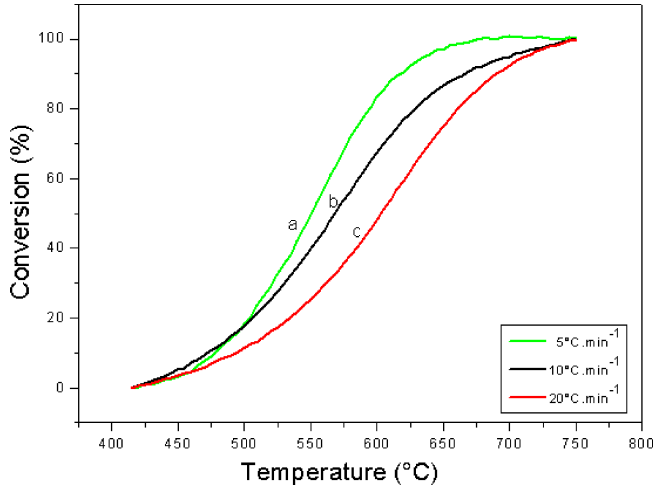

Fig. 12. Conversion curves vs.Temperature for thermal of coke in SAPO-11: a – 5°C.min^{-1}, b – 10°C.min^{-1}, c – 20°C.min^{-1}

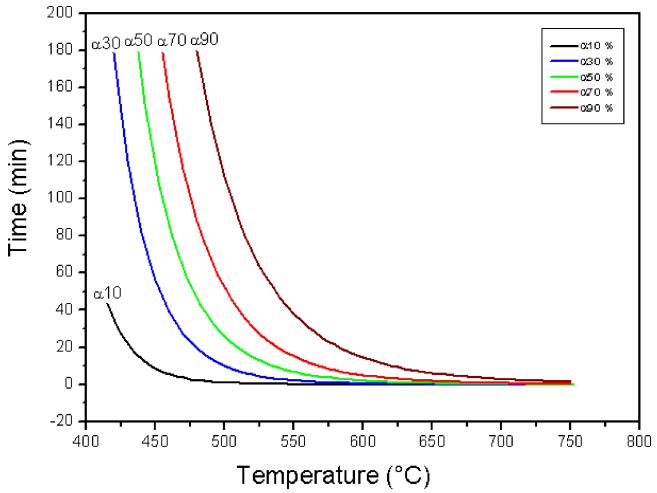

Fig. 13. Conversion curves for SAPO-11

4. Conclusions

SAPO-11 molecular sieves were obtained successfully by synthesis through the hydrothermal media, afterwards they were submitted to characterizations through: XRD, SEM, N_2 Adsorption Desorption, FT-IR and TG/DTG under specific conditions such as, undergoing calcination to remove the diisopropylamine template from the micropores of the catalyst. The obtained results confirm that the sample has a high cristallinity, viewed through the typical peaks in XRD diffraction patterns, the morphological aspect shows a predominantly microporous structure due to its orthorhombic geometry mingled with some pseudo-spherical aggregates and a high specific surface area with a majority of internal surface area, showing the adequacy of the synthesis route used. SAPO-11 had a good catalytic performance, it was observed in all cases in the first 10 min of reaction showed the highest conversion rates, falling sharply to reach stability usually after 20 min of reaction. The obtained products from the cracking of n-hexane catalytic tests were: propane, isobutane, 1-butene, n-butane, 2-butene-trans, cis-2-butene, isopentane, n-pentane, being preferential the isopentene formation. Based on the distribution of obtained products indicates a predominance of olefinic products (1-butene, 2-butene-trans and cis-2-butene), and high n-butane/isobutane ratio indicating that isomerization reactions of n-butane chain occurred on a small scale. This could also be confirmed through viewing the selectivity graphs of products, where the isopentene always appears as a product obtained in smaller quantities. Regarding the ratio 2-butene-trans/cis-2-butene, it could also be observed in most cases the following rule of selectivity: 2-butene-trans $>$ cis-2-butene $>$ 1-butene. Consequently, SAPO-11 molecular sieves would be of great interest for potential application in catalytic reactions due to their high standards of deactivation/regenerability.

Acknowledgements. This work was financially supported by grants from the Brazilian agency CAPES and the PPGEM of the Federal University of Rio Grande do Norte/Brazil, thus the authors wish to acknowledge their support.

REFERENCES

[1] S.T. Wilson, B.M. Lok, C.A. Messina, T.R. Cannan, and E.M. Flanigen, "Aluminophosphate molecular sieves: a new class of microporous crystalline inorganic solids", *J. Am. Chem. Soc.* 104, 1146–1147 (1982).

[2] B.M. Lok, C.A. Messina, R.L. Patton, R.T. Gajek, T.R. Cannan, and E.M. Flanigen,"Silicoaluminophosphate molecular sieves: another new class of microporous crystalline inorganic solids", *J. Am. Chem. Soc.* 106, 6092–6093 (1984).

[3] C.M. Lopez, F.J. Machado, J. Goldwasser, B. Mendez, K. Rodriguez, and M.M. Ramirezagudelo, "The successive crystallization and characterization of SAPO-31 and SAPO-11 from the same synthesis gel – influence on the selectivity for 1-butene isomerization", *Zeolites* 19, 133–141 (1997).

[4] A.K. Sinha and S. Seelan, "Characterization of SAPO-11 and SAPO-31 synthesized from aqueous and non-aqueous media", *Appl. Catal.* A. 270, 245–252 (2004).

[5] B.M. Lok, C.A. Messina, R.L. Patton, R.T. Gajek, T.R. Cannan, and E.M. Flanigen, "Crystalline silicoaluminophosphates", *US Patent*, 4440871, (1984).

[6] E.M. Flanigen, B.M. Lok, R.T. Patton, and S.T. Wilson, "Aluminophosphate molecular sieves and the periodic table", *Proc. 7^{th} Int. Zeolite Conf.* 1, 103–112 (1986).

[7] A.S. Araujo, J.C. Diniz, A.O.S. Silva, and R.A.A. Melo, "Hydrothermal synthesis of cerium aluminophosphate", *J. Alloys Compd.* 250, 532–535 (1997).

[8] N. Rajic, V. Kaucic, and D. Stojakovic, "Synthesis and characterization of the CoSAPO-14 and CoSAPO-34", *Zeolites* 10, 169–173 (1990).

[9] G. Nardin, L. Randaccio, N. Rajik, and V. Kaucic, "The structure of CoSAPO-34, containing i-propylamine as a template", *Zeolites* 11, 192–194 (1991).

[10] R. Wang, C.F. Lin, Y.S. Ho, L.J. Leu, and K.J. Chao, "Silicon species in a SAPO-5 molecular sieve", *Appl. Catal.* A 72, 39–49 (1991).

[11] D. Goldfarb, "MAS n.m.r and e.s.r. studies of MnALPO5", *Zeolites* 9, 509–515 (1989).

[12] A.M. Prakash and S. Unnikrishnan, "Synthesis of SAPO-34: high silicon incorporation in the presence of morpholine as template", *J. Chem. Soc. Faraday Trans.* 90, 2291–2296 (1994).

[13] J. Tan, Z. Liu, X. Bao, X. Liu, X. Han, C. He, and R. Zhai, "Crystallization and Si incorporation mechanisms of SAPO-34", *Micropor. Mesopor. Mater*. 53, 97–108 (2002).

[14] Ø.B. Vistad, D.E. Akporiaye, F. Taulelle, and K.P. Lillerud, "In Situ NMR of SAPO-34 crystallization", *Chem. Mater.* 15, 1639–1649 (2003).

[15] H.O. Pastore, S. Coluccia, and L. Marchese, "Porous aluminophosphates: from molecular sieves to designed acid catalysts", *Annu. Rev. Mater. Res.* 35, 351–395 (2005).

[16] B.M. Lok, T.R. Cannan, and C.A. Messina, "The role of organic molecules in molecular sieve synthesis", *Zeolites* 3, 282–291 (1983).

[17] R. Vomscheid, M. Briend, M.J. Peltre, and D. Barthomeuf, "Reversible interaction of NH_3 with the framework of template-free zeolite-type SAPO-34", *J. Chem. Soc. Faraday Trans.* 91, 3281–3284 (1995).

[18] P. Meriaudeau, V.A. Tuan, V.T. Nghiem, S.Y. Lai, L.N. Hung, and C. Naccache, "SAPO-11, SAPO-31 and SAPO-41 molecular sieves: synthesis, characterization, and catalytic properties in n-octane hydroisomerization", *J. Catal.* 169, 55–66 (1997).

[19] J.M. Campelo, F. Lafont, and J.M. Marinas, "Hydroisomerization and hydrocracking of n-hexane on Pt/SAPO-5 and Pt/SAPO-11", *Zeolites* 15, 97–103 (1995).

[20] M. Alfonzo, J. Goldwasser, C.M. Lopez, F.J. Machado, M. Matjushin, and B. Méndez, "Effect of the synthesis conditions on the crystallinity and surface acidity of SAPO-11", *J. Mol. Catal.* A 98, 35–48 (1995).

[21] S. Vyazovkin, "Modification of the integral isoconversional method to account for variation in the activation energy", *J. Computational Chemistry* 22, 178–183 (2001).

[22] S. Vyazovkin and C.A. Wright, "Model-free and model-fitting approaches to kinetic analysis of isothermal and nonisothermal data", *Thermochim. Acta* 340, 53–68 (1999).

[23] A.I. Biaglow, A.T. Adamo, G.T Kokotailo, and R.J. Gorte, "An examination of the acid sites in SAPO-5", *J. Catal.* 131, 252–259 (1991).

[24] S. Zhang, S. Chen, P. Dong, G. Yuan, and K. Xu, "Characterization and hydroisomerization performance of SAPO-11 molecular sieves synthesized in different media", *Appl. Catal.* A. 332, 46–55 (2007).

[25] A.K. Sinha, S. Sainkar and S. Sivasanker, "An improved method for the synthesis of the silicoaluminophosphate molecular sieves, SAPO-5, SAPO-11 and SAPO-31", *Micropor. Mesopor. Mater* 31, 321–331 (1999).

[26] J.H. de Boer, D.H. Everett, and F.S. Stone, *The Structure and Properties of Porous Materials*, pp. 68–94, Butterworth, London, 1958.

[27] S. Chen and G. Manos, "In situ thermogravimetric study of coke formation during catalytic cracking of normal hexane and 1-hexene over ultrastable Y zeolite", *J. Catal.* 226, 343–350 (2004).